IEEE Access
Multidisciplinary | Rapid Review | Open Access Journal

Received 16 January 2023, accepted 2 February 2023, date of publication 6 February 2023, date of current version 13 February 2023.

Digital Object Identifier 10.1109/ACCESS.2023.3242917

RESEARCH ARTICLE

Residual Compensation-Based Extreme Learning Machine for MIMO-NOMA Receiver

M. REZWANUL MAHMOOD[1], MOHAMMAD ABDUL MATIN[1], (Senior Member, IEEE), PANAGIOTIS SARIGIANNIDIS[2], (Member, IEEE), SOTIRIOS K. GOUDOS[3], (Senior Member, IEEE), AND GEORGE K. KARAGIANNIDIS[4], (Fellow, IEEE)

[1]Department of Electrical and Computer Engineering, North South University, Dhaka 1229, Bangladesh
[2]Department of Informatics and Telecommunications Engineering, University of Western Macedonia, 501 00 Kozani, Greece
[3]ELEDIA@AUTH, Department of Physics, Aristotle University of Thessaloniki, 54124 Thessaloniki, Greece
[4]Department of Electrical and Computer Engineering, Aristotle University of Thessaloniki, 54124 Thessaloniki, Greece

Corresponding author: Mohammad Abdul Matin (mohammad.matin@northsouth.edu)

This work was supported by the European Union's Horizon 2020 Research and Innovation Program (TERMINET) under Grant 957406.

ABSTRACT Extreme learning machine (ELM) uses a simple machine learning (ML) architecture that allows its implementation for smart IoT network operations. However, some inaccuracy lies between the predicted and the actual data during the ELM training, which can be caused due to the limitation of the modeling representation. This paper thus investigates a residual compensation-based ELM (RC-ELM) for its application in designing a receiver for MIMO-NOMA aided IoT systems. In RC-ELM, the base ELM layers determine the relationship between the transmitted and received data and the additional layers of the RC-ELM attempt to compensate the error introduced during the training mechanism. The analysis of the appropriate number of compensation layers for training error minimization is conducted on the basis of the bit error rate (BER) and the error vector magnitude (EVM) performances of the RC-ELM training. A minimum BER improvement of 5% for user 1 and 18% for user 2 is shown with with the aid of RC-ELM for a two-IoT user instance. The EVM is marginally increased by 0.0008% for user 1 and 1.61% for user 2 in training stage. Besides, the RC-ELM receiver is also compared to the minimum mean square error (MMSE), the classic ELM and the trained multilayer perceptron (MLP) receivers in terms of BER and EVM. Both of the ELM receivers show improved performances with respect to the other receivers.

INDEX TERMS IoT, MIMO-NOMA, machine learning, extreme learning machine, RC-ELM, multilayer perceptron.

I. INTRODUCTION

The deployment of 5G/B5G has created the opportunity to realize Internet of Things (IoT) into reality. Since the popularity of the internet is ever increasing, the growth of the number of communication devices is escalating exponentially. Thus, multiple access technology is being brought into attention for massive access provision to IoT devices. However, accommodating large number of smart IoT devices within a given bandwidth and ensuring QoS parameters such as low latency and high throughput at the same time can be a challenging task. Non-orthogonal multiple access (NOMA) is seen a promising enabling technology to address this issue [1]. In orthogonal multiple access (OMA), the users are allocated with orthogonal time/frequency resources. On the contrary, in NOMA, the users are allocated with same frequency resources at the same time. Thus, massive accessibility with increased throughput and lower latency is ensured. By combining NOMA with multiple-input multiple-output (MIMO), enhanced spectral efficiency is also achieved. MIMO-NOMA has thus received much interest in research domain and industrial applications to enhance the IoT network performance.

Generally, power domain NOMA is adopted for multiple access provision. Multiple users with different power

The associate editor coordinating the review of this manuscript and approving it for publication was Bilal Khawaja.

allocations are accommodated in same time and frequency resources. Later, the signals from multiple sources are superimposed and transmitted to the desired destination. However, this leads to the inter-user interference problem since the time and frequency resources utilized by the users are non-orthogonal, and consequently complicates the extraction of the required information from the received signal. Thus, several studies are being conducted on MIMO-NOMA signal processing, which includes channel estimation, signal detection and interference cancellation operations. In [2], a zero-forcing (ZF) beamforming is studied for multi-user downlink MIMO-NOMA system where each cluster contains two single-antenna user devices. Channel state information (CSI) of each cluster-head is extracted for the ZF beamforming design. Maximum-likelihood based receiver is utilized in [3] for uplink MIMO-NOMA to detect quadrature phase shift keying (QPSK) modulated symbols. A precoding scheme, which focuses on minimization of transmission power consumption, is suggested in [4] where the transmitted signal is recovered with the help of the precoder and the minimum mean square error (MMSE) equalizer. An iterative linear MMSE (LMMSE) is designed in [5] multiuser detection in MIMO-NOMA system. The mismatch between LMMSE detection and decoding is attempted to remove in the study for better signal recovery and achievable rate is then analyzed. The performance of these approaches depends on the accuracy of the channel estimation. Besides, the inter-user interference mitigation approaches required in MIMO-NOMA also relies on channel information-based techniques [6]. However, parameters such as auto-covariance of the channel and noise variance are challenging to obtain in practical communication systems [7]. One possible approach can be the adoption of machine learning (ML) techniques to conduct such signal processing mechanisms [8].

Several studies on ML algorithm such as deep neural network (DNN)-based approaches are conducted for MIMO-NOMA systems to detect signals [9], [10], [11]. DNN based precoding and decoding approaches are proposed in [9] for MIMO-NOMA system with successive interference cancellation (SIC) scheme. Uplink signal detection for MIMO-NOMA is performed by means of convolutional neural networks (CNN) in [10]. The iterative soft-thresholding technique is the foundation of the adaptive DL-based receiver architecture known as MMNet [11]. The performance of the MMNet receiver is evaluated for massive MIMO (mMIMO) channel with spatial correlation. However, the tuning of DNN parameters such as weights and biases are performed by means of iterative mechanisms, which may complicate the implementation of such DNN algorithms. Contrary to the tuning mechanism-based ML algorithms, extreme learning machine (ELM) uses randomly assigned input weights and biases (that connect between the input layer and the hidden layer) and perform supervised learning with the help of training datasets by determining the output weights (connecting the hidden layer and the output layer), which is responsible for determining the desired output. In [12] and [13], the ELM-based receiver systems are proposed which do not require any channel information. However, due to the limitation of modeling representation, some training inaccuracy may be introduced during the learning stage as ML approaches, including ELM, might not always reach the global minima with the given ML parameters. Thus regularization technique is applied to ensure that the ML algorithms perform well when generalized. A residual compensation-based ELM (RC-ELM) is proposed for building the MIMO-NOMA receiver in order to reduce training error. To our knowledge, this is the first time an RC-ELM has been researched in relation to creating a MIMO-NOMA receiver. The following highlights the paper's contribution.

- An RC-ELM-based receiver is presented for a multi-user MIMO-NOMA aided IoT system. The base ELM layers are used to map the transmitted and received data, whereas the additional layers are used to compensate the error introduced during training. A bit error rate (BER) analysis of choosing the effective number of compensation layers to mitigate training error by means of the RC-ELM receiver is conducted.
- The performance of the proposed ELM receiver is contrasted with that of the MMSE, multilayer perceptron (MLP) and classic ELM receivers. It is demonstrated that both of the ELM receivers provides better BER than the MMSE and the MLP receivers.

The paper is organized as follows. Section II discusses the MIMO-NOMA system model, which includes data transmission and reception, channel estimation and signal detection with linear receiver. Section III discusses the basics of ELM-based receiver and section IV discusses the RC-ELM receiver. Section V presents the simulation parameters and discussions on the results. Section VI concludes the paper.

Notations: Matrix is represented by the bold uppercase letters, vector is represented by bold lowercase letters and scalar variables are represented by small letters. The inverse, transpose, conjugate transpose and Moore-Penrose inverse operations are denoted by $(.)^{-1}$, $(.)^{T}$, $(.)^{*}$ and $(.)^{\dagger}$ respectively. The matrix inverse operation with regularization parameter is represented by $(.)$. Activation function is represented by $G(.)$. The Frobenius norm of a matrix is denoted by $||.||_F$.

II. SYSTEM MODEL

A. MIMO-NOMA DATA TRANSMISSION AND RECEPTION

A visual representation of the downlink MIMO-NOMA system is presented in Fig. 1. The source data bits for the IoT user k are digitally modulated. Afterwards, inverse discrete Fourier transformation (IDFT) of the data symbols of each IoT user is carried out, followed by cyclic prefix (CP) addition. Each user is allocated with power p_k and multiplied with the respective signals. Later, the respective signals are added. After that, the superposed data transferred to the receiver

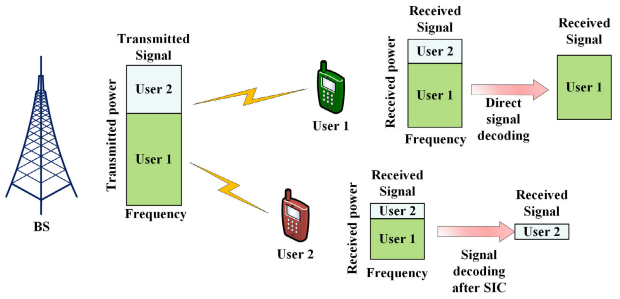

FIGURE 1. MIMO-NOMA system diagram.

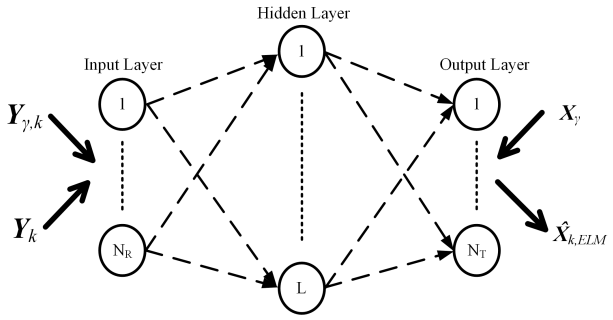

FIGURE 2. Classic ELM neural network.

through wireless channel [14]. After receiving the superposed data by each IoT user, CP is removed and discrete Fourier transformation (DFT) is carried out. The received DFT symbols can be mathematically expressed as shown in (1).

$$\boldsymbol{Y}_k = \boldsymbol{F}_k \boldsymbol{X} + \boldsymbol{Z}_k \tag{1}$$

Here, $\boldsymbol{Y}_k \in \mathbb{C}^{N_R \times N}$ is the received symbol matrix by the user k, N_R is the number of receiving antennas and N is the number of subcarriers. $\boldsymbol{F}_k \in \mathbb{C}^{N_R \times N_T}$ is the channel matrix for user k, where $\boldsymbol{F}_k = \frac{1}{\sqrt{d_k}}\boldsymbol{H}_k$, $\boldsymbol{H}_k$ follows Rayleigh distribution and d_k is the distance between the BS and the user k. $\boldsymbol{X} \in \mathbb{C}^{N_T \times N}$ is the superposed signal transmitted by the BS with N_T transmitting antennas and $\boldsymbol{X} = \sum_{k=1}^{K} \sqrt{p_k}\boldsymbol{X}_k$, where p_k is the power allocated to the user k. $\boldsymbol{Z}_k$ is the added noise with power $\sigma^2_{\boldsymbol{Z}_k}$.

B. CHANNEL ESTIMATION AND EQUALIZATION WITH LINEAR RECEIVER

Channel estimation is performed by means of transmitted and received reference symbols. If the transmitted and received reference symbols are represented by $\boldsymbol{X}_\gamma$ and $\boldsymbol{Y}_{\gamma,k}$, then according to (1),

$$\boldsymbol{Y}_{\gamma,k} = \boldsymbol{F}_k \boldsymbol{X}_\gamma + \boldsymbol{Z}_k \tag{2}$$

Generally, channel is estimated in practical communication network by means of LS estimation method due to its computational simplicity [7]. The LS estimation of the channel $\hat{\boldsymbol{F}}_k$ is determined as follows [15].

$$\hat{\boldsymbol{F}}_{k,LS} = (\boldsymbol{X}^*_\gamma \boldsymbol{X}_\gamma)^{-1}\boldsymbol{X}^*_\gamma \boldsymbol{Y}_{\gamma,k} = \boldsymbol{X}^\dagger_\gamma \boldsymbol{Y}_{\gamma,k} \tag{3}$$

A Bayesian-based MMSE estimation method can be used to reduce the average mean square error (MSE) of the LS estimation of the channel [16], [17].

$$\hat{\boldsymbol{F}}_{k,MMSE} = \sigma^2_{\hat{\boldsymbol{F}}_{k,LS}}(\sigma^2_{\hat{\boldsymbol{F}}_{k,LS}} + \sigma^2_{\boldsymbol{Z}_k})^{-1}\hat{\boldsymbol{F}}_{k,LS} \tag{4}$$

Here, $\sigma^2_{\hat{\boldsymbol{F}}_{k,LS}}$ is the estimated channel variance. Since, MMSE approach provides better estimation of the channel, $\hat{\boldsymbol{F}}_{k,MMSE}$ is chosen for performing the equalization operation. The MMSE equalization is expressed as follows.

$$\hat{\boldsymbol{X}}_{k,MMSE} = (\hat{\boldsymbol{F}}^*_{k,MMSE}\hat{\boldsymbol{F}}_{k,MMSE} + \sigma^2_{\boldsymbol{Z}_k}\boldsymbol{I})^{-1}\hat{\boldsymbol{F}}^*_{k,MMSE}\boldsymbol{Y}_k \tag{5}$$

The user with highest power can directly decode its own signal and the user with low power needs to perform SIC operation. Each user receives their desired data bits after executing digital demodulation.

III. CLASSIC EXTREME LEARNING MACHINE (ELM) FOR MIMO-NOMA SYSTEM

The classic ELM-based receiver for the MIMO-NOMA system is presented in this section. Instead of tuning the input weights by back-propagation algorithms, the input weights as well as the biases, that connect the input layer and the hidden layer, are randomly chosen. The output weights, that connect the hidden layer and the output layer, are determined in the training stage of ELM. Keeping the input weights and biases unchanged in testing stage, the received data symbols are processed to obtain the transmitted data.

The working principle of the ELM algorithm is demonstrated in Fig. 2. Training of ELM algorithm is required prior to its implementation, which is performed with the help of transmitted-received reference symbol pairs. At first, the received reference symbols $\boldsymbol{Y}_{\gamma,k}$ are fed into the input layer, with input neurons is equal to N_R. The hidden layer output $\boldsymbol{M}_{\gamma,k} \in \mathbb{C}^{L \times N}$ is determined with the help of the activation function $G(.)$. The output layer neuron weight parameter $\boldsymbol{\beta}_{0,k} \in \mathbb{C}^{L \times N_T}$ is then determined from the transmitted reference symbols $\boldsymbol{X}_\gamma$ and $\boldsymbol{M}_{\gamma,k}$. The following mathematical equations state the training mechanism of ELM.

$$\boldsymbol{M}_{\gamma,0,k} = G(\boldsymbol{W}_k \boldsymbol{Y}_{\gamma,k} + \boldsymbol{b}_k) \tag{6}$$

$$\begin{aligned}\boldsymbol{\beta}_{0,k} &= (\boldsymbol{M}^*_{\gamma,0,k}\boldsymbol{M}_{\gamma,0,k} + \alpha\boldsymbol{I})^{-1}\boldsymbol{M}^*_{\gamma,0,k}\boldsymbol{X}_\gamma \\ &= \acute{\boldsymbol{M}}_{\gamma,0,k}\boldsymbol{X}_\gamma\end{aligned} \tag{7}$$

In the equation (6) and (7), subscript $(.)_\gamma$ refers to terms associated with reference signals. $\boldsymbol{W}_k \in \mathbb{C}^{L \times N_R}$ and $\boldsymbol{b}_k \in \mathbb{C}^{L \times 1}$ are input weight and bias parameters respectively which are randomly chosen and kept constant once assigned. The symbol α, in (7), is the regularization parameter and used to solve the least square problem $\boldsymbol{\beta}_{0,k} = argmin_{\boldsymbol{\beta}_{0,k}} ||\boldsymbol{M}_{\gamma,0,k}\boldsymbol{\beta}_{0,k} - \boldsymbol{X}_\gamma||$ [18].

Symbol detection is executed in testing stage. The hidden layer output $\boldsymbol{M}_{0,k}$ is computed with the received data symbols $\boldsymbol{Y}_k$ as shown in (8). The detected symbols are obtained

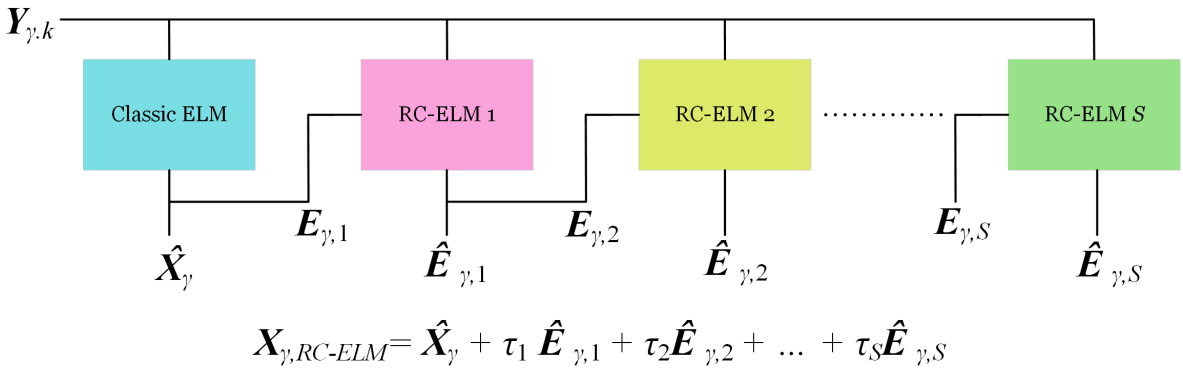

FIGURE 3. RC-ELM network training stage block diagram.

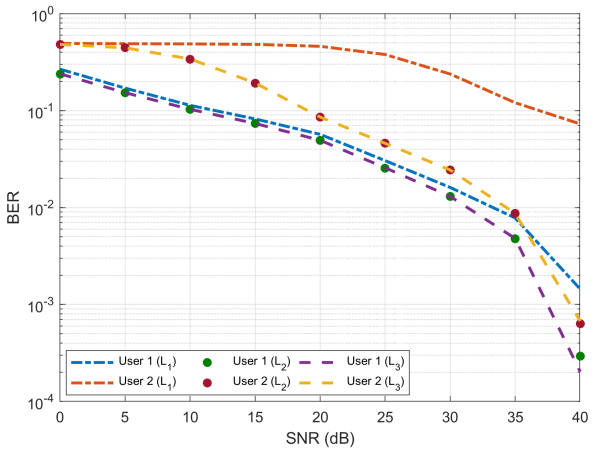

FIGURE 4. BER vs. SNR for the classic ELM receiver as a function of different hidden layer neurons.

from (9).

$$\boldsymbol{M}_{0,k} = G(\boldsymbol{W}_k \boldsymbol{Y}_k + \boldsymbol{b}_k) \tag{8}$$

$$\hat{\boldsymbol{X}}_{k,ELM} = \boldsymbol{\beta}_{0,k}^T \boldsymbol{M}_{0,k} \tag{9}$$

Here, $\hat{\boldsymbol{X}}_{k,ELM}$ denotes the ELM detected symbols. It is to be noted that detection by means of ELM algorithm takes place without determining the channel matrix directly. It directly removes the channel effect from the received data by performing online training with the help of the transmitted and the received reference symbols.

IV. RESIDUAL COMPENSATION-BASED ELM (RC-ELM) RECEIVER FOR MIMO-NOMA

Though the classic ELM is an effective ML algorithm for regression or classification, some error may exist in the training of the algorithm. Suppose, $\boldsymbol{X}$ is the actual data and $\hat{\boldsymbol{X}}_{k,ELM}$ is the predicted symbols with the help of the ELM receiver. The estimation error can then be expressed as follows.

$$\begin{aligned} \boldsymbol{E} &= \boldsymbol{X} - \hat{\boldsymbol{X}}_{k,ELM} \\ &= \boldsymbol{X} - \boldsymbol{\beta}_{0,k}^T \boldsymbol{M}_{0,k} \end{aligned} \tag{10}$$

Algorithm 1 Summary of RC-ELM Receiver Design Mechanism

TRAINING OF ELM

Input: $\boldsymbol{Y}_{\gamma,k}$, $\boldsymbol{X}_\gamma$
Random assignment of the input weight $\boldsymbol{W}_k$ and the bias $\boldsymbol{b}_k$
Computation of the hidden layer neuron parameter $\boldsymbol{M}_{\gamma_k}$ from (6)
Determination of output weight $\boldsymbol{\beta}_{0,k}$ from (7)
Computation of $\hat{\boldsymbol{E}}_{\gamma,s}$ from (15) and τ_s from (17) for s^{th} compensation layer[1]

TESTING OF ELM
Input: $\boldsymbol{Y}_k$, τ_s, and $\hat{\boldsymbol{E}}_{\gamma,s}$
Computation of hidden layer neuron parameter $\boldsymbol{M}$ from (8)

Determination of $\hat{\boldsymbol{X}}_{k,ELM}$ from (9)
Determination of $\hat{\boldsymbol{X}}_{k,RC-ELM}$ from (18)

The first compensation layer operation will always be performed according to (11) -(12).

In order to reduce this error occurred in the training stage, the RC-ELM receiver is presented in this paper. In RC-ELM [19], additional components (which are known as compensation layers) are added to the classic ELM layers, as shown in Fig. 3. In the input of each compensation layer, $\boldsymbol{Y}_{\gamma,k}$ is provided as input. The reference symbols $\boldsymbol{Y}_{\gamma,k}$, if were used in (8), then the expression in (9) would provide an estimated output $\hat{\boldsymbol{X}}_\gamma$. According to (10), the error between the actual reference symbols and the ELM equalized symbols could be written as

$$\boldsymbol{E}_{\gamma,1} = \boldsymbol{X}_\gamma - \hat{\boldsymbol{X}}_\gamma = \boldsymbol{X}_\gamma - \boldsymbol{\beta}_{0,k}^T \boldsymbol{M}_{\gamma,0,k} \tag{11}$$

$\boldsymbol{E}_{\gamma,1}$ represents the training error. The first compensation layer performs the estimation of $\boldsymbol{E}_{\gamma,1}$ according to the

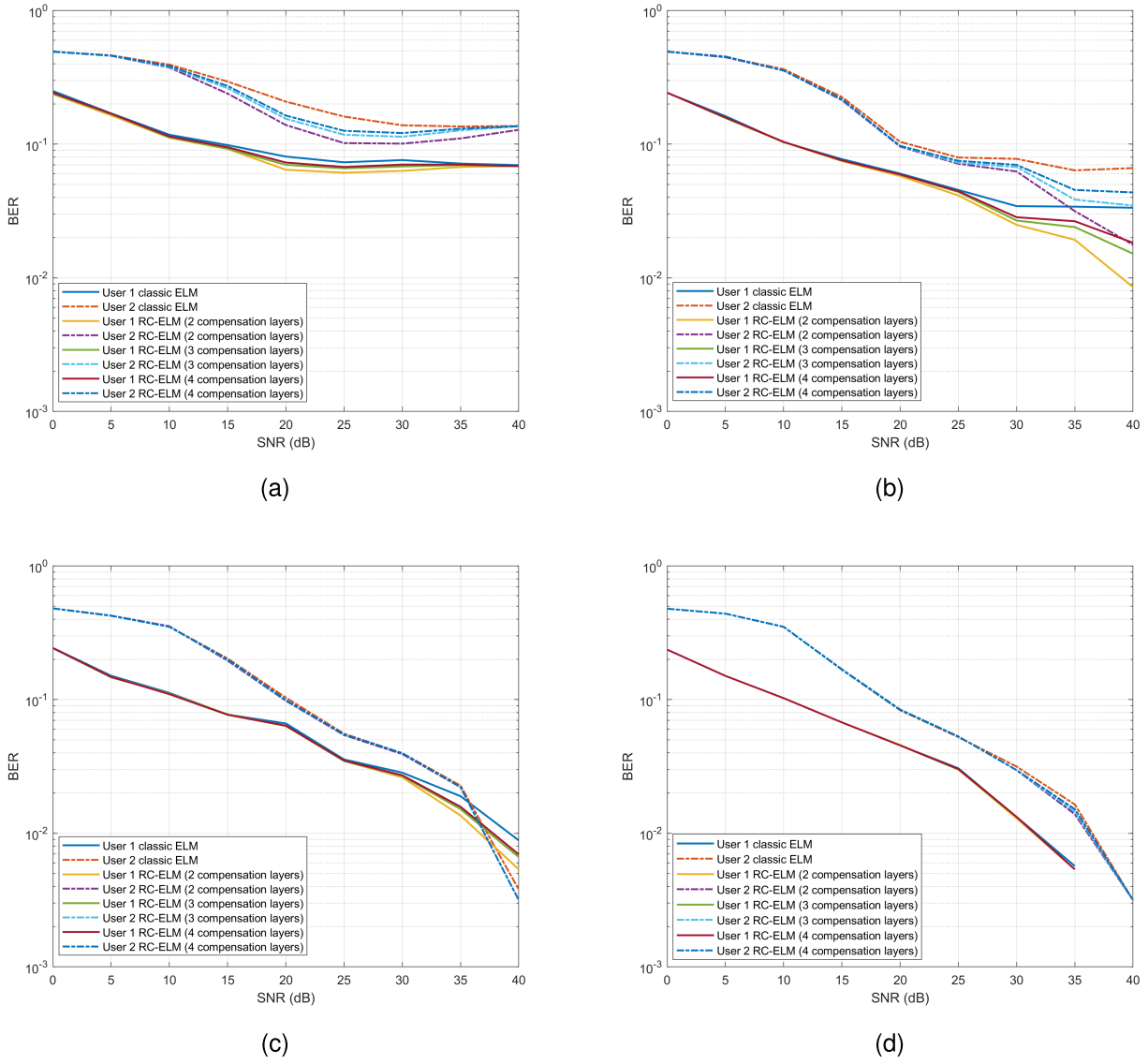

FIGURE 5. BER for ELM and RC-ELM-based MIMO-NOMA receivers in training stage with (a) $\alpha = 10^{-2}$ (b) $\alpha = 10^{-3}$ (c) $\alpha = 10^{-4}$ (d) $\alpha = 10^{-5}$.

following equation.

$$\begin{aligned}\hat{\boldsymbol{E}}_{\gamma,1} &= \boldsymbol{\beta}_{1,k}^{T}\boldsymbol{M}_{\gamma,1,k} \\ &= ((\boldsymbol{M}_{\gamma,1,k}^{*}\boldsymbol{M}_{\gamma,1,k} + \alpha\boldsymbol{I})^{-1}\boldsymbol{M}_{\gamma,1,k}^{*}\boldsymbol{E}_{\gamma,1})^{T}\boldsymbol{M}_{\gamma,1,k} \\ &= (\acute{\boldsymbol{M}}_{\gamma,1,k}(\boldsymbol{X}_{\gamma} - \hat{\boldsymbol{X}}_{\gamma}))^{T}\boldsymbol{M}_{\gamma,1,k} \qquad (12)\end{aligned}$$

Here, $\boldsymbol{E}_{\gamma,1}$ is the target output in the first compensation layer. The first layer prediction inaccuracy $\boldsymbol{E}_{\gamma,2}$ is then determined by

$$\boldsymbol{E}_{\gamma,2} = \boldsymbol{E}_{\gamma,1} - \hat{\boldsymbol{E}}_{\gamma,1}. \qquad (13)$$

In the second compensation layer, considering $\boldsymbol{E}_{\gamma,2}$ as the desired output, the RC-ELM training is executed as follows.

$$\begin{aligned}\hat{\boldsymbol{E}}_{\gamma,2} &= \boldsymbol{\beta}_{2,k}^{T}\boldsymbol{M}_{\gamma,2,k} \\ &= ((\boldsymbol{M}_{\gamma,2,k}^{*}\boldsymbol{M}_{\gamma,2,k} + \alpha\boldsymbol{I})^{-1}\boldsymbol{M}_{\gamma,2,k}^{*}\boldsymbol{E}_{\gamma,2})^{T}\boldsymbol{M}_{\gamma,2,k} \\ &= (\acute{\boldsymbol{M}}_{\gamma,2,k}(\boldsymbol{E}_{\gamma,1} - \hat{\boldsymbol{E}}_{\gamma,1}))^{T}\boldsymbol{M}_{\gamma,2,k} \\ &= (\acute{\boldsymbol{M}}_{\gamma,2,k}((\boldsymbol{X}_{\gamma} - \hat{\boldsymbol{X}}_{\gamma}) - \hat{\boldsymbol{E}}_{\gamma,1}))^{T}\boldsymbol{M}_{\gamma,2,k} \qquad (14)\end{aligned}$$

TABLE 1. Simulation parameters.

Parameters	Value/Technique
MIMO configuration $N_R \times N_t$	2×4
Number of IoT users, K	2
Number of BS	1
Modulation format	16QAM
Transmission power	30 dBm
SNR (dB)	0-50
Number of PRB	66
Number of subcarrier per PRB	12
Carrier frequency	30 GHz
Subcarrier spacing	120 kHz
Number of OFDM symbols per slot	14

TABLE 2. EVM vs SNR of the classic ELM and the RC-ELM receivers in training stage for different regularization parameters.

SNR	0	5	10	15	20	25	30	35	40
Classic ELM ($\alpha = 10^{-2}$)									
User 1	45.114	29.823	20.021	14.816	13.061	12.416	12.175	12.103	12.083
User 2	127.732	123.888	111.104	102.550	98.885	95.732	93.653	93.593	91.100
RC-ELM (2 compensation layer, $\alpha = 10^{-2}$)									
User 1	44.477	28.247	17.367	10.732	8.013	7.048	7.060	7.743	8.491
User 2	126.553	123.761	107.657	98.470	91.615	82.686	79.169	84.808	88.493
RC-ELM (3 compensation layer, $\alpha = 10^{-2}$)									
User 1	44.639	28.653	18.074	11.903	9.574	8.823	8.871	9.447	10.028
User 2	127.104	122.967	108.863	100.016	94.687	87.198	87.897	91.532	89.807
RC-ELM (4 compensation layer, $\alpha = 10^{-2}$)									
User 1	44.739	28.904	18.502	12.579	10.423	9.736	9.753	10.210	10.659
User 2	127.299	123.426	109.398	101.168	95.789	89.804	90.158	92.788	90.486
Classic ELM ($\alpha = 10^{-3}$)									
User 1	47.025	29.796	18.694	10.226	6.386	3.681	2.350	1.734	1.488
User 2	130.967	119.235	111.465	101.717	86.476	77.847	74.934	74.215	72.942
RC-ELM (2 compensation layer, $\alpha = 10^{-3}$)									
User 1	45.911	28.630	18.096	10.042	6.253	3.484	2.034	1.276	0.912
User 2	131.023	119.546	112.073	99.887	85.209	71.845	63.463	54.721	43.401
RC-ELM (3 compensation layer, $\alpha = 10^{-3}$)									
User 1	46.124	28.769	18.135	10.062	6.281	3.535	2.120	1.409	1.091
User 2	130.745	119.864	111.027	100.430	85.127	74.827	68.944	61.480	55.948
RC-ELM (4 compensation layer, $\alpha = 10^{-3}$)									
User 1	46.283	28.886	18.169	10.076	6.298	3.565	2.171	1.484	1.186
User 2	130.479	119.737	111.504	100.906	85.072	75.486	72.080	66.331	57.889
Classic ELM ($\alpha = 10^{-4}$)									
User 1	46.734	27.228	15.665	8.910	4.999	2.837	1.640	0.929	0.552
User 2	128.916	122.963	108.064	94.954	76.873	64.013	45.737	31.478	1.840
RC-ELM (2 compensation layer, $\alpha = 10^{-4}$)									
User 1	46.734	27.228	15.665	8.908	4.996	2.827	1.632	0.919	0.536
User 2	128.917	122.964	108.067	94.970	76.892	63.522	45.112	31.484	1.829
RC-ELM (3 compensation layer, $\alpha = 10^{-4}$)									
User 1	46.734	27.228	15.665	8.909	4.997	2.829	1.633	0.921	0.540
User 2	128.917	122.964	108.066	94.965	76.886	63.976	45.107	31.481	1.832
RC-ELM (4 compensation layer, $\alpha = 10^{-4}$)									
User 1	46.734	27.228	15.665	8.909	4.997	2.830	1.634	0.923	0.542
User 2	128.917	122.964	108.065	94.962	76.883	64.428	45.104	31.480	1.833
Classic ELM ($\alpha = 10^{-5}$)									
User 1	44.410	26.927	15.175	8.769	5.014	2.848	1.594	0.879	0.506
User 2	128.073	121.317	110.258	94.977	82.919	66.085	54.708	40.223	14.876
RC-ELM (2 compensation layer, $\alpha = 10^{-5}$)									
User 1	44.410	26.927	15.175	8.769	5.014	2.848	1.593	0.878	0.505
User 2	128.140	121.319	109.772	95.962	82.937	65.282	53.795	37.451	12.920
RC-ELM (3 compensation layer, $\alpha = 10^{-5}$)									
User 1	44.410	26.927	15.175	8.769	5.014	2.848	1.593	0.878	0.505
User 2	128.139	121.318	110.263	95.963	83.259	65.689	53.776	37.449	12.920
RC-ELM (4 compensation layer, $\alpha = 10^{-5}$)									
User 1	44.410	26.927	15.175	8.769	5.014	2.848	1.593	0.878	0.505
User 2	128.139	121.318	110.262	95.963	83.255	66.096	53.763	37.447	12.920

Thus the s^{th} compensation layer operation (where, $s = 1, 2, \ldots, S$) in RC-ELM can be generally represented as

$$\hat{\boldsymbol{E}}_{\gamma,s} = \boldsymbol{\beta}_{s,k}^{T} \boldsymbol{M}_{\gamma,k}, \tag{15}$$

where, $\boldsymbol{\beta}_{s,k} = (\boldsymbol{M}_{\gamma,s,k}^{*} \boldsymbol{M}_{\gamma,s,k} + \alpha \boldsymbol{I})^{-1} \boldsymbol{M}_{\gamma,s,k}^{*} \boldsymbol{E}_{\gamma,s} = \acute{\boldsymbol{M}}_{\gamma,s,k} \boldsymbol{E}_{\gamma,s}$ and $\boldsymbol{E}_{\gamma,s} = \boldsymbol{E}_{\gamma,s-1} - \hat{\boldsymbol{E}}_{\gamma,s-1}$. The output of the RC-ELM in the training stage would be expressed as follows.

$$\hat{\boldsymbol{X}}_{\gamma,RC-ELM} = \hat{\boldsymbol{X}}_{\gamma} + \tau_1 \hat{\boldsymbol{E}}_{\gamma,1} + \tau_2 \hat{\boldsymbol{E}}_{\gamma,2} + \cdots + \tau_S \hat{\boldsymbol{E}}_{\gamma,S} \tag{16a}$$

$$= \hat{\boldsymbol{X}}_{\gamma} + \sum_{s=1}^{S} \tau_s \hat{\boldsymbol{E}}_{\gamma,s} \tag{16b}$$

Here, τ_s represents the weights of each compensation layer which fulfills the criteria $\sum_{s=1}^{S} \tau_s = 1$. The compensation layer weights can be calculated as follows.

$$\tau_s = \frac{\frac{1}{||\boldsymbol{E}_{\gamma,s} - \hat{\boldsymbol{E}}_{\gamma,s}||_F}}{\sum_{s=1}^{S} \frac{1}{||\boldsymbol{E}_{\gamma,s} - \hat{\boldsymbol{E}}_{\gamma,s}||_F}} \tag{17}$$

In the testing stage, the estimated errors and the compensation layer weights are used. After performing equalization

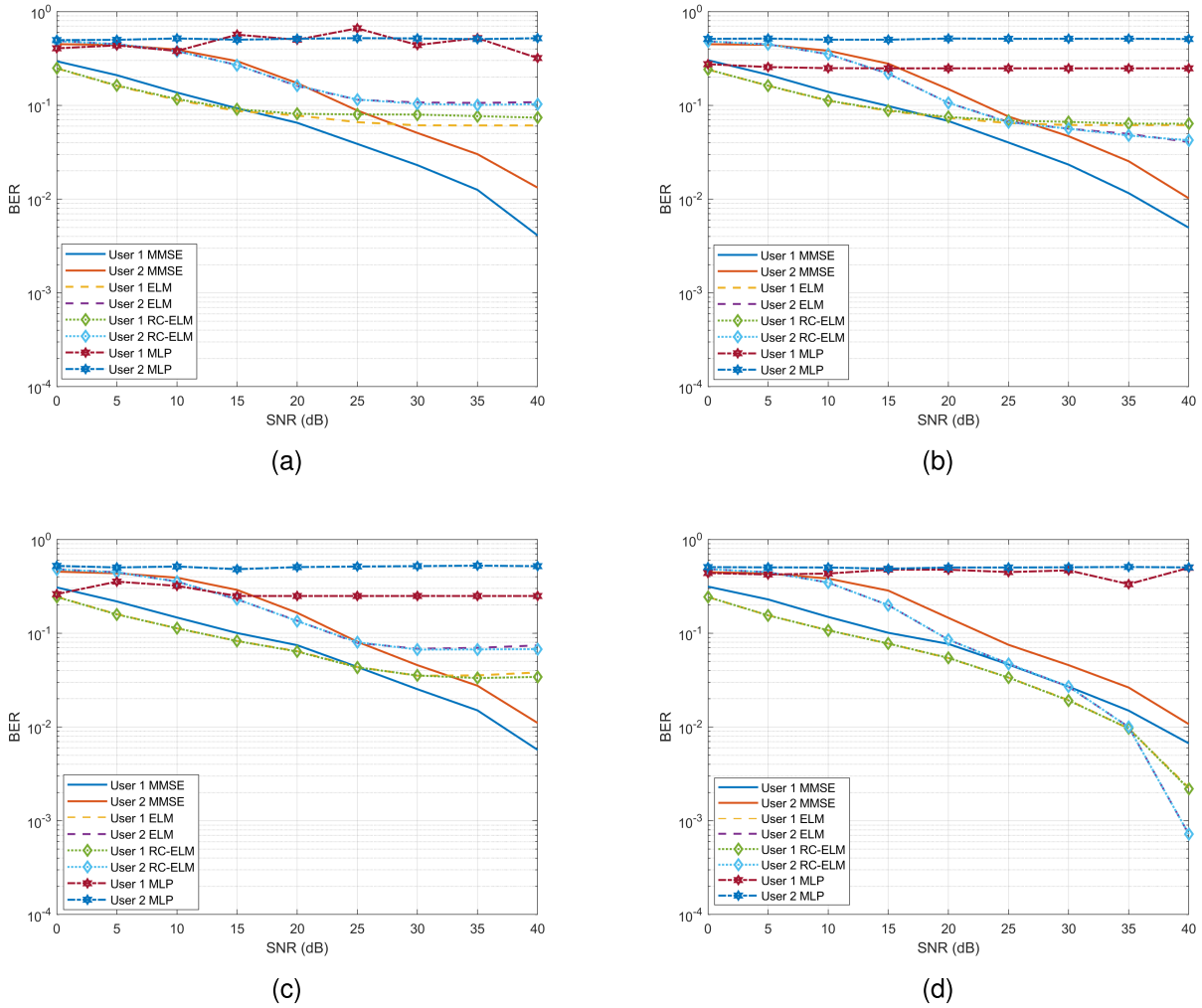

FIGURE 6. BER for MMSE, MLP, ELM and RC-ELM-based MIMO-NOMA receivers (in testing stage with (a) $\alpha = 10^{-2}$ (b) $\alpha = 10^{-3}$ (c) $\alpha = 10^{-4}$ (d) $\alpha = 10^{-5}$).

according to (9), the final output by means of RC-ELM for the IoT user k can be represented as follows.

$$\hat{\boldsymbol{X}}_{k,RC-ELM} = \hat{\boldsymbol{X}}_{k,ELM} + \sum_{s=1}^{S} \tau_s \hat{\boldsymbol{E}}_{\gamma,s} \tag{18}$$

The mechanism of the RC-ELM receiver is summarized in Algorithm 1.

V. SIMULATION RESULTS

This section presents the simulation results for MIMO-NOMA communication system operating at 30 GHz carrier frequency. The user 1 and user 2 are respectively at the distances 20 m and 10 m apart from the BS. The transmission power is considered to be 30 dBm and the values of p_1 and p_2 for user 1 and user 2 are respectively 0.92 and 0.08. Normalized 16-quadrature amplitude modulation (16-QAM) is chosen in our study. Transmitted data are organized in physical resource block (PRB) arrangement [12]. The transmitted and received reference symbols at one OFDM symbol time are considered for channel estimation as well as the online training of both of the ELM receivers and the MLP receiver. The parameters of simulation are stated in Table 1.

To design both the ELM receivers, activation function *tanh* is used [12], [13]. The input weights $\boldsymbol{W}$ and biases $\boldsymbol{b}$ follow uniform distribution within the interval [-0.01,0.01]. The input layer in both the ELM receivers consists of 2 neurons (each neuron takes the symbols received at each antenna) and the output layer consists of 4 neurons (each neuron takes the symbols transmitted from each antenna). Fig. 4 demonstrates the BER obtained by adopting the classic ELM-based receiver with different hidden layer neurons, which are $L_1 = 2$, $L_2 = 4$ and $L_3 = 8$. It is observed that the BER for L_2 and L_3 is superior to that for L_1. Besides, the difference in BER values for L_2 and L_3 is almost negligible in all SNR values. For simplicity, $L_2 = 4$ is chosen in this study for both of the classic ELM and the RC-ELM receivers.

TABLE 3. EVM performance of MMSE, MLP, classic ELM and RC-ELM receivers (in testing stage for different regularization parameters).

SNR	0	5	10	15	20	25	30	35	40
MMSE									
User 1	110.562	52.055	32.148	20.966	13.71	10.67	5.382	2.711	1.595
User 2	293.536	141.744	122.59	101.899	88.089	72.782	59.499	42.971	27.917
MLP									
User 1	164.653	166.454	170.906	135.689	92.724	167.884	168.269	155.838	152.643
User 2	106.954	108.428	109.209	109.37	108.12	108.907	110.219	110.849	110.053
Classic ELM ($\alpha = 10^{-2}$)									
User 1	47.068	30.679	19.157	11.993	8.005	5.928	5.136	4.835	4.728
User 2	130.228	124.465	113.331	100.481	94.405	92.786	94.189	99.026	101.332
RC-ELM (2 compensation layer, $\alpha = 10^{-2}$)									
User 1	46.939	30.683	19.091	12.015	8.086	6.083	5.311	5.023	4.898
User 2	130.35	124.404	113.178	100.588	93.955	91.211	89.881	91.655	92.664
Classic ELM ($\alpha = 10^{-3}$)									
User 1	44.602	27.325	15.671	8.928	5.073	2.904	1.684	1.099	0.809
User 2	130.255	123.489	109.456	98.478	88.551	79.345	75.446	74.869	73.636
RC-ELM (2 compensation layer, $\alpha = 10^{-3}$)									
User 1	44.603	27.324	15.675	8.927	5.076	2.908	1.700	1.121	0.838
User 2	130.350	123.627	109.780	97.803	88.320	79.510	74.205	71.641	72.264
Classic ELM ($\alpha = 10^{-4}$)									
User 1	44.837	27.134	15.511	8.895	5.041	2.850	1.600	0.898	0.516
User 2	130.845	123.838	109.345	99.084	90.607	79.279	70.281	63.313	52.863
RC-ELM (2 compensation layer, $\alpha = 10^{-4}$)									
User 1	44.837	27.133	15.512	8.899	5.043	2.850	1.601	0.898	0.516
User 2	130.569	123.713	109.487	99.132	89.783	79.359	69.518	62.693	53.099
Classic ELM ($\alpha = 10^{-5}$)									
User 1	44.850	27.137	15.611	8.872	5.056	2.913	1.687	0.957	0.549
User 2	130.999	123.093	109.548	97.125	80.412	65.184	52.280	33.963	11.131
RC-ELM (2 compensation layer, $\alpha = 10^{-5}$)									
User 1	44.850	27.137	15.611	8.874	5.063	2.919	1.688	0.956	0.549
User 2	130.952	123.091	109.551	97.196	80.249	65.535	51.971	34.316	11.309

Fig. 5 demonstrates the BER obtained by the classic ELM receiver and the RC-ELM receiver in training stage with 2, 3 and 4 compensation layers. As the regularization parameter α varies from 10^{-2} to 10^{-5}, the BER performance improves with the increase of SNR. The RC-ELM receiver is able to provide lower BER than the classic ELM. The RC-ELM with 2 compensation layers shows lower BER with respect to the RC-ELM with 3 and 4 compensation layers. In Fig. 5d, the BER values of the classic ELM receiver is very similar to that of the RC-based receiver, although marginal improvement is observed in high SNR values. For instance, at SNR = 35 dB, compared to the classic ELM receiver, the RC-ELM provides about 5% lower BER for user 1 and about 18% lower BER for user 2. Table 2 presents the EVM performance (determined on the basis of the Euclidean distance between the equalized symbols and the reference constellation symbols) of the classic ELM and the RC-ELM receivers with training symbols. Overall, RC-ELM with 2 compensation layers shows descent performance with respect to the classic ELM receiver as well as the RC-ELM receivers with 3 and 4 compensation layers. For user 1, compared to the classic ELM, the EVM performance improvement with RC-ELM with 2 compensation layers, within $25 - 30$ dB SNR, for $\alpha = 10^2, 10^3, 10^4$ and 10^5 are observed to be 4.7%, 0.34%, 0.01% and 0.0008% respectively. For user 2, the EVM performance, for $\alpha = 10^2, 10^3, 10^4$ and 10^5, is improved by 9.2%, 13.5%, 0.28% and 1.61% within the same SNR values. Based on the BER and the EVM performances observed with the reference symbols, the number of compensation layers in RC-ELM in testing stage is chosen to be 2.

An MLP-based receiver is also implemented in this study for performance comparison [20]. A three hidden layer incorporated-MLP algorithm is trained online in order to detect the real and imaginary part of the received symbols. For each part, the number of neurons in each layer is 4, 8 and 6 respectively. Similar to the ELM receivers, the number of input layer and output layer is respectively chosen to be equal to 2 and 4. Activation function *tanh* is also considered for the MLP receiver at each hidden layer and the weight parameters are updated with the learning rate of 0.005 and momentum of 0.8. Fig. 6 presents the BER obtained by the MMSE, the trained classic and the RC-ELMs as well as the MLP receivers. For all the values of α, both of the ELM receivers provide better performance than the MLP receivers. For $\alpha = 10^{-5}$, the BER performances by both of the ELM receivers are almost identical. Even the ELM receivers show improved performance against the MMSE receiver. At the BER value of about 10^{-2}, about 2.5 dB and 5 dB gains are observed

by the ELM receivers (with respect to the MMSE receiver) for user 1 and user 2 respectively. Table 3 presents the EVM performance of the MMSE and the ML algorithms (in testing stage). The ELM receivers shows better performance for $\alpha = 10^{-5}$.

The accuracy of the channel estimation determines the inter-user interference mitigation and as a result, the recovery of the signal in NOMA-based communication networks. Thus, any error in the channel estimation will affect the overall signal recovery process by means of the linear receiver, since such receiver utilize the estimated channel information. On the other hand, ELM receiver does not require to directly estimate channel. It rather uses the reference symbols to perform signal detection and minimize the interference. Contrary to the complicated structure of the MLP algorithm-based approach, ELM does not require tuning of input weights and biases, which simplifies its application. The addition of the compensation layers in ELM for RC-ELM receiver may increase complications. However, it is able to minimize the error caused in the training of the ELM algorithm, which is reflected by the BER and the EVM analyses in training stage.

VI. CONCLUSION

An RC-ELM based receiver is studied in this paper for designing a receiver for the MIMO-NOMA aided IoT system. The proposed receiver uses the classic ELM algorithm for equalizing the symbols and the additional compensation layers are used to minimize the errors introduced in the classic ELM training. The BER and the EVM analyses of both of the ELM receivers in training stage is conducted. The performance of the RC-ELM is also compared to the MMSE, classic ELM and MLP receivers. In terms of BER and EVM, It is shown that both of the ELM receivers have shown improved performance against the MMSE and the MLP receivers. Furthermore, it is shown that the RC-ELM receiver training is more reliable than the conventional ELM training. The automatic estimation of the RC-compensation ELM's layer count in order to enhance the performance of its input-output mapping could be a future research target using RC-ELM.

REFERENCES

[1] S. M. R. Islam, N. Avazov, O. A. Dobre, and K.-S. Kwak, "Power-domain non-orthogonal multiple access (NOMA) in 5G systems: Potentials and challenges," *IEEE Commun. Surveys Tuts.*, vol. 19, no. 2, pp. 721–742, 2nd Quart., 2017.

[2] B. Kimy, S. Lim, H. Kim, S. Suh, J. Kwun, S. Choi, C. Lee, S. Lee, and D. Hong, "Non-orthogonal multiple access in a downlink multiuser beamforming system," in *Proc. IEEE Mil. Commun. Conf. (MILCOM)*, Nov. 2013, pp. 1278–1283.

[3] J. S. Yeom, H. S. Jang, K. S. Ko, and B. C. Jung, "BER performance of uplink NOMA with joint maximum-likelihood detector," *IEEE Trans. Veh. Technol.*, vol. 68, no. 10, pp. 10295–10300, Oct. 2019.

[4] H. Wang, R. Zhang, R. Song, and S.-H. Leung, "A novel power minimization precoding scheme for MIMO-NOMA uplink systems," *IEEE Commun. Lett.*, vol. 22, no. 5, pp. 1106–1109, May 2018.

[5] L. Liu, Y. Chi, C. Yuen, Y. L. Guan, and Y. Li, "Capacity-achieving MIMO-NOMA: Iterative LMMSE detection," *IEEE Trans. Signal Process.*, vol. 67, no. 7, pp. 1758–1773, Apr. 2019.

[6] E. N. Tominaga, O. L. A. López, H. Alves, R. D. Souza, and J. L. Rebelatto, "Performance analysis of MIMO-NOMA iterative receivers for massive connectivity," *IEEE Access*, vol. 10, pp. 46808–46822, 2022.

[7] J. Liu, K. Mei, X. Zhang, D. Ma, and J. Wei, "Online extreme learning machine-based channel estimation and equalization for OFDM systems," *IEEE Commun. Lett.*, vol. 23, no. 7, pp. 1276–1279, Jul. 2019.

[8] M. Yao, M. Sohul, V. Marojevic, and J. H. Reed, "Artificial intelligence defined 5G radio access networks," *IEEE Commun. Mag.*, vol. 57, no. 3, pp. 14–20, Mar. 2019.

[9] J.-M. Kang, I.-M. Kim, and C.-J. Chun, "Deep learning-based MIMO-NOMA with imperfect SIC decoding," *IEEE Syst. J.*, vol. 14, no. 3, pp. 3414–3417, Sep. 2020.

[10] L. Chuan, C. Qing, and L. Xianxu, "Uplink NOMA signal transmission with convolutional neural networks approach," *J. Syst. Eng. Electron.*, vol. 31, no. 5, pp. 890–898, 2020.

[11] M. Khani, M. Alizadeh, J. Hoydis, and P. Fleming, "Adaptive neural signal detection for massive MIMO," *IEEE Trans. Wireless Commun.*, vol. 19, no. 8, pp. 5635–5648, Aug. 2020.

[12] D. F. Carrera, D. Zabala-Blanco, C. Vargas-Rosales, and C. A. Azurdia-Meza, "Extreme learning machine-based receiver for multi-user massive MIMO systems," *IEEE Commun. Lett.*, vol. 25, no. 2, pp. 484–488, Feb. 2021.

[13] D. F. Carrera, C. Vargas-Rosales, D. Zabala-Blanco, N. M. Yungaicela-Naula, C. A. Azurdia-Meza, M. Marey, and A. D. Firoozabadi, "Novel multilayer extreme learning machine as a massive MIMO receiver for millimeter wave communications," *IEEE Access*, vol. 10, pp. 58965–58981, 2022.

[14] Y. Tian, G. Pan, and M.-S. Alouini, "On NOMA-based mmWave communications," *IEEE Trans. Veh. Technol.*, vol. 69, no. 12, pp. 15398–15411, Dec. 2020.

[15] Y. S. Cho, J. Kim, W. Y. Yang, and C. G. Kang, *MIMO-OFDM Wireless Communications With MATLAB*. Singapore: Wiley, 2010.

[16] D. F. Carrera, C. Vargas-Rosales, N. M. Yungaicela-Naula, and L. Azpilicueta, "Comparative study of artificial neural network based channel equalization methods for mmWave communications," *IEEE Access*, vol. 9, pp. 41678–41687, 2021.

[17] D. F. Carrera, C. Vargas-Rosales, L. Azpilicueta, and J. A. Galaviz-Aguilar, "Comparative study of channel estimators for massive MIMO 5G NR systems," *IET Commun.*, vol. 14, no. 7, pp. 1175–1184, Apr. 2020.

[18] D. Gao and Q. Guo, "Extreme learning machine-based receiver for MIMO LED communications," *Digit. Signal Process.*, vol. 95, Dec. 2019, Art. no. 102594.

[19] J. Zhang, W. Xiao, Y. Li, and S. Zhang, "Residual compensation extreme learning machine for regression," *Neurocomputing*, vol. 311, pp. 126–136, Oct. 2018.

[20] L. Noriega, "Multilayer perceptron tutorial," School Comput., Staffordshire Univ., Stoke-on-Trent, U.K., Tech. Rep., 2005.

M. REZWANUL MAHMOOD received the B.S. degree in electrical and electronic engineering (EEE) from East West University, Dhaka, Bangladesh, in 2017. He is currently pursuing the M.S. degree in electrical and electronic engineering (EEE) with North South University, Dhaka. He is currently working as a Research Assistant with North South University. He has published few papers in reputed journals and international conference. His research interests include future wireless networks, the Internet of Things, and machine learning.

MOHAMMAD ABDUL MATIN (Senior Member, IEEE) received the B.Sc. degree in electrical and electronic engineering from BUET, Bangladesh, the M.Sc. degree in digital communication from Loughborough University, U.K., and the Ph.D. degree in wireless communication from Newcastle University, U.K. He has been a Professor with the Department of Electrical and Computer Engineering, North South University (NSU), since 2008. He has published over 120 peer-reviewed journals and conference papers. He is the author/editor of 17 academic books and 21 book chapters. He serves as a member for the Editorial Board for several international journals, including *IEEE Communications Magazine* and *IET Wireless Sensor Systems*. He has received a number of prizes and scholarships, including the Best Student Prize (Loughborough University), Commonwealth Scholarship, and Overseas Research Scholarship (ORS) conferred by the Committee of Vice Chancellors and Principals (CVCP) in the U.K.

PANAGIOTIS SARIGIANNIDIS (Member, IEEE) received the B.Sc. and Ph.D. degrees in computer science from the Aristotle University of Thessaloniki, Thessaloniki, Greece, in 2001 and 2007, respectively. He is currently the Director of the ITHACA Laboratory (https://ithaca.ece.uowm.gr/), the Co-Founder of the first spinoff of the University of Western Macedonia: MetaMind Innovations P.C. (https://metamind.gr), and an Associate Professor with the Department of Electrical and Computer Engineering, University of Western Macedonia, Kozani, Greece. He has published over 220 papers in international journals, conferences, and book chapters, including IEEE Communications Surveys and Tutorials, IEEE Transactions on Communications, IEEE Internet of Things Journal, IEEE Transactions on Broadcasting, IEEE Systems Journal, *IEEE Wireless Communications* magazine, IEEE Open Journal of the Communications Society, IEEE/OSA Journal of Lightwave Technology, IEEE Access, and *Computer Networks*. His research interests include telecommunication networks, the Internet of Things, and network security. He participates in the editorial boards of various journals.

SOTIRIOS K. GOUDOS (Senior Member, IEEE) received the B.Sc. degree in physics, the M.Sc. degree in electronics, and the Ph.D. degree in physics from the Aristotle University of Thessaloniki, in 1991, 1994, and 2001, respectively, the master's degree in information systems from the University of Macedonia, Greece, in 2005, and the Diploma degree in electrical and computer engineering from the Aristotle University of Thessaloniki, in 2011. He joined the Department of Physics, Aristotle University of Thessaloniki, in 2013, where he is currently an Associate Professor. His research interests include antenna and microwave structures design, evolutionary algorithms, wireless communications, and semantic web technologies. He is also the Director of the ELEDIA@AUTH Laboratory and a member of the ELEDIA Research Center Network. He is also the Founding Editor-in-Chief of the *Telecom* Open Access Journal (MDPI). He is also serving as an Associate Editor for IEEE Transactions on Antennas and Propagation, IEEE Access, and IEEE Open Journal of the Communication Society. He is also serving as the IEEE Greece Section Secretary. He is the author of the book *Emerging Evolutionary Algorithms for Antennas and Wireless Communications*, Institution of Engineering and Technology, in 2021. He is a member of the IEICE, the Greek Physics Society, the Technical Chamber of Greece, and the Greek Computer Society.

GEORGE K. KARAGIANNIDIS (Fellow, IEEE) was born in Pithagorion, Samos Island, Greece. He received the University Diploma (five years) and Ph.D. degrees in electrical and computer engineering from the University of Patras, in 1987 and 1999, respectively. From 2000 to 2004, he was a Senior Researcher with the Institute for Space Applications and Remote Sensing, National Observatory of Athens, Greece. In June 2004, he joined as the Faculty Member with the Aristotle University of Thessaloniki, Greece, where he is currently a Professor with the Electrical and Computer Engineering Department and the Head of the Wireless Communications and Information Processing (WCIP) Group. He is also an Honorary Professor with Southwest Jiaotong University, Chengdu, China. His research interests include the broad area of digital communications systems and signal processing, with emphasis on wireless communications, optical wireless communications, wireless power transfer and applications and communications, and signal processing for biomedical engineering. He has been involved as the general chair, the technical program chair, and a member of technical program committees in several IEEE and non-IEEE conferences. In the past, he was an editor of several IEEE journals. From 2012 to 2015, he was the Editor-in-Chief of IEEE Communications Letters. Currently, he serves as the Associate Editor-in-Chief for IEEE Open Journal of the Communications Society. He is one of the highly-cited authors across all areas of electrical engineering, recognized from Clarivate Analytics as a Web of Science Highly-Cited Researcher in the seven consecutive years (2015–2021).